Global Ecology & Biogeography (2000) **9**, 481–497

RESEARCH ARTICLE

Impact of ENSO on East African ecosystems: a multivariate analysis based on climate and remote sensing data

P. D. PLISNIER, S. SERNEELS* and E. F. LAMBIN* *Royal Museum for Central Africa, Geology & Mineralogy Department, Leuvensesteenweg, 13, B-3080 Tervuren, Belgium. E-mail: pierre-denis.plisnier@arcadis.be *Department of Geography, Université Catholique de Louvain, Place Louis Pasteur, 3, B-1348 Louvain-la-Neuve, Belgium*

ABSTRACT

1 The El Niño-Southern Oscillation (ENSO) is an important driver of inter-annual variations in climate and ecosystem productivity in tropical regions. Most previous studies have analysed ENSO-induced changes in climate based on a single variable, such as rainfall. Also, it is generally assumed that the ENSO impact in East Africa is geographically uniform.

2 The objective of this study is to improve understanding of the impact of ENSO on East African ecosystems, by measuring teleconnections between an ENSO index and a number of ecosystem variables in a spatially explicit way and for different time lags. We analysed the spatial patterns of teleconnections in the region by combining time series of climate variables measured for meteorological stations with time series of a vegetation index and surface temperature data measured by remote sensing.

3 Our results confirm the ENSO impact on the climatic and ecological variability in East Africa. However, the pattern of teleconnections is much more complex than generally assumed, both in terms of spatial distribution and impact on different ecosystem variables. Not all climate and land surface variables are teleconnected to ENSO in the same way, which leads to a complex impact of ENSO on the ecosystem. Moreover, the ENSO impact is highly differentiated in space, as the direction, magnitude and timing of this impact are controlled by the local climate system, the presence of large lakes, proximity to the coast and, possibly, local topography and land cover.

Key words Climate, East Africa, El Niño, ENSO, land cover, NDVI, remote sensing, teleconnections.

INTRODUCTION

Inter-annual climatic variations in tropical regions are in part influenced by the El Niño-Southern Oscillation (ENSO) (Houghton *et al.*, 1990). Modelling experiments have been conducted to forecast ENSO several months ahead (Chen *et al.*, 1995). In areas such as East Africa, where agriculture and fisheries are largely influenced by climate variability, understanding the teleconnections between ENSO, weather patterns and the ecosystem productivity could have important beneficial effects for resource management (Cane *et al.*, 1994; Verdin *et al.*, 1999) or public health (Linthicum *et al.*, 1999). By teleconnections, one means linkages over great distance of seemingly disconnected weather anomalies.

In previous studies, ENSO-induced changes in weather patterns in distant regions have often been investigated based on a single variable (e.g. rainfall or a remotely sensed vegetation index). To describe more comprehensively such teleconnections and their impact on ecosystem functions (e.g. crop or fish production), one has to recognize the multidimensional character of this impact. Actually, ENSO affects a range of linked climate and ecosystem variables whose

combined effect has an impact on resources and socio-economic activities. The impact of ENSO on a given ecosystem thus has to be measured on a set of variables. Moreover, the spatial and temporal coherence of the response of these ecosystem variables to ENSO has to be investigated to evaluate the differentiated impact of ENSO on different subregions and vegetation formations. Actually, the response of different climatic and ecosystem variables to ENSO might occur with different time lags and might be spatially heterogeneous. While most previous studies have generally assumed that the ENSO impact in East Africa was uniform in space and on all ecosystem variables, the reality is likely to be more complex. For example, Linthicum *et al.* (1999) recently noted that, in East Africa, the pattern of ENSO teleconnections can be irregular and a region-wide effect cannot usually be found.

The objective of this study is to improve understanding of the impact of ENSO on East African ecosystems, by measuring teleconnections between an ENSO index and a number of ecosystem variables in East Africa in a spatially explicit way and for different time lags, and by analysing the spatial patterns of teleconnections in the region. This paper seeks to add to the general understanding of climate and vegetation interactions in eastern Africa.

BACKGROUND

Most of the previous investigations on the climate teleconnections in East Africa have been based on rainfall data (Nicholson & Entekhabi, 1986; Ogallo, 1987; Ropelewski & Halpert, 1987; Farmer, 1988). Nicholson (1996) used time series of rainfall data from 1901 to 1985. She found that most of the peaks in rainfall in East Africa correspond to warm ENSO years in the Pacific Ocean, e.g. 1941, 1951, 1957, 1963, 1968, 1972 and 1982. During warm ENSO events, wetter conditions are observed near the equator while drier conditions are observed in southern Africa (Rasmusson & Arkin, 1985; Ropelewski & Halpert, 1987).

Besides rainfall, teleconnection studies with other climatic variables, such as air temperature and air pressure, have generally been included in studies at a global scale. Those studies have shown that, during warm ENSO events, air temperature is higher in most of the tropics (Diaz & Kiladis, 1992) while air pressure is higher in East Africa (Trenberth & Shea, 1987). There has been no detailed study of teleconnections with ENSO in the East African region that has dealt with air temperature and humidity, although those are important factors for agriculture (directly or through their influence on pests). Inter-annual and seasonal variations in these climatic variables may have an impact on crop yields. Regions situated at the boundary between two biomes or ecosystems, such as semi-arid regions, are particularly sensitive to small changes in air temperature or humidity. Small changes in air temperature may also affect the thermal stability of water columns of lakes. For the Great Lakes of the African Rift, this may have a significant impact on the mixing conditions of the waters and on the primary production patterns, which might then affect fish productivity (Gucinski *et al.*, 1990).

Over the past few years, several authors have studied time–series of satellite images to assess the response of vegetation to inter-annual climatic variability. To investigate the existence of an ENSO signal, authors have correlated a vegetation index NDVI (the normalized difference vegetation index) with ENSO indicators measured in the southern Pacific Ocean. Anyamba & Eastman (1996) used standardized principal components analysis to demonstrate a link between time series of NDVI data in Africa and ENSO phenomena. They found a positive correlation between the 8th principal component of the African NDVI time series, and both Pacific southern oscillation index (SOI) and outgoing long-wave radiation (OLR) anomalies. They found the effect to be most pronounced in Southern Africa. However, the 8th principal component accounts for less than 1% of the total variance of the NDVI time series. Note that several authors have indicated that a relationship exists between NDVI values for African vegetation and rainfall (Davenport & Nicholson, 1993; Eklundh, 1998; Richard & Poccard, 1998).

Recently, global scale vegetation index data were linked with sea surface temperature (SST) anomalies for warm and cool ENSO events

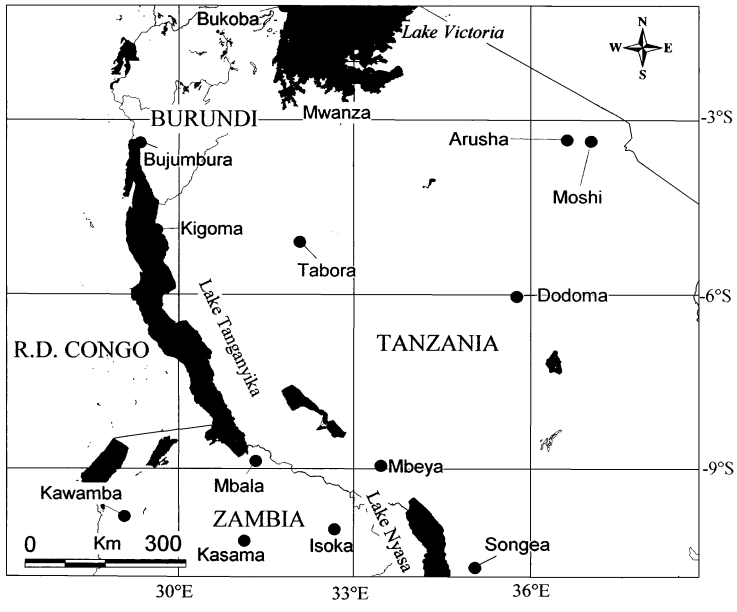

Fig. 1 Study area with the location of the meteorological stations used in this study.

(Myneni *et al.*, 1996). The similarity between the monthly SST and NDVI anomalies time series was determined by calculating the correlation coefficient at a fine spatial resolution. Three areas of Africa were identified as having a strong correlation between Pacific SST and coincident NDVI anomalies: parts of eastern Africa extending towards the Horn of Africa, south-eastern Africa, and central southern Africa. Eastern Africa and the Horn of Africa showed a tendency towards wetter conditions with tropical Pacific SST warming, whereas the other areas experienced drought conditions with the ENSO warming. In another tropical region, Batista *et al.* (1997) recently found evidence of the influence of El Niño phenomena on the vegetation cover in the Amazonian region of northern Brazil. These authors state that ENSO has a multiyear impact on the vegetation. A decrease in vegetation due to ENSO-related droughts requires 2 years for full recovery to pre-ENSO NDVI values in northern Brazil.

STUDY AREA

The study area comprises the zone between 26°50′E–38°24′E and 0°05′N–11°04′S. This area is centred on Lake Tanganyika. The boundaries are shown in Fig. 1.

The topography of the area is characterized by a central and western plateau in Tanzania situated at an altitude between 1000 and 1500 m. In the north, Lake Victoria lies at 1134 m altitude while, in the west, Lake Tanganyika (773 m) and Lake Nyasa (=) (473 m) occupy the Rift Valley, surrounded by high ranges of mountains. Although East Africa has an equatorial position, it is a region of widespread rainfall deficiency. In our study area, annual rainfall exceeds 1500 mm only in the Lake Victoria area. Near the equator, most of the stations have two rainfall seasons: the long rains (March–May) and the short rains (October–December). These are associated with the Intertropical Convergence Zone (ITCZ). In the southern part of the study area, a single rainy season is observed as almost all the rains fall between September and April. Rainfall patterns are influenced by altitude and topography. Two main wind systems are observed: the northern monsoon, from December to March, and the south-easterlies, from June to October.

The north-western part of the study area is covered with evergreen tropical forest, gradually

changing into woody savanna and, towards the south, in a mixture of cultivation with savanna vegetation. In the north, the evergreen forest changes into a mixture of cropland and natural vegetation going towards Lake Victoria. The central plateau mainly consists of savanna, some grasslands and woody savanna near Lake Tanganyika. Between Lake Rukwa and Lake Nyasa, there is a cultivated area, while the south-eastern part of the study area is a mixture of savanna and woody savanna vegetation. The vegetation description is based on the IGBP land cover map for Africa (Loveland & Belward, 1999) and can be found on the internet at: http://edcwww.cr.usgs.gov/landdaac/glcc/tablambert_af.html

DATA

Remote sensing data

The study is based on the NOAA/NASA Pathfinder Advanced Very-High Resolution Radiometer (AVHRR) 8-km Land Data Set (Smith *et al.*, 1997). The spatial resolution of this database is 8 by 8 km. It covers the period from 1981 to 1994. The dataset contains 12 variables from which we derived two biophysical indicators: normalized difference vegetation index (NDVI, calculated from radiance values in channels 1 and 2) and surface brightness temperature (Ts) computed from AVHRR channels 4 and 5 brightness temperatures. Brightness temperatures were derived by inverting the Plank equation. Land surface temperature (Ts) was then derived through the split window method for land surfaces, assuming a constant emissivity (Price, 1984). More detailed information on the processing of PAL data is available in Smith *et al.* (1997). Empirical studies and simulations with radiative transfer models support the interpretation of the NDVI in terms of fraction of photosynthetically active radiation absorbed by the vegetation canopy, canopy attributes (e.g. green biomass or green leaf area index), state of the vegetation (i.e. vegetation vigour or stress) and instantaneous rates associated with the activity of the vegetation (e.g. Kumar and Monteith, 1981; Asrar *et al.*, 1992; Myneni *et al.*, 1996). Surface temperature is related to surface moisture availability and evapotranspiration, as a function of latent heat flux (Carlson *et al.*, 1990). To remove cloud influence and minimize off-nadir views, monthly maximum value compositing was applied to the data (Holben, 1986), selecting the maximum value of daily NDVI over a 1-month period. The Ts value for the date corresponding to the maximum NDVI was also retained.

As the Global AVHRR remote sensing data are only available since the early 1980s, the period of analysis of both the remote sensing and climate data has been limited to 1981 until 1994. This period includes three warm ENSO events, in 1982–83, 1986–87 and 1991–94. One cold event (La Niña) was observed in 1989–90.

Climate data

Meteorological monthly data were obtained from the Departments of Meteorology in Zambia, Tanzania and Burundi. Only the stations where more than 90% of the data were available for the study period were used (Fig. 1). This forced us to work with a limited number of stations. However, neighbouring stations generally behave similarly and the patterns detected in this study are robust by comparison with the stations providing a lower availability of data. The following variables have been analysed: rainfall, relative air humidity, monthly average of maximum (T_{max}) and minimum temperature (T_{min}), and average air temperature [calculated as $(T_{max} + T_{min})/2$]. The time–series for maximum air temperature in Mwanza was incomplete, with data missing for 1989 and 1990. For this station, the maximum and average air temperature data for the period 1975–88 were used in the analysis. Rainfall data for Tanzania were computed as total values per season: October to December (short rains), December to February (short dry season), and March to May (long rains). The analyses of rainfall data were therefore performed at a higher level of temporal aggregation than the other variables.

An additional variable combining remote sensing measurements and ground observations was computed: infrared remote sensing data combined with maximum air temperature data can be used to assess water conditions of the vegetation at a regional scale. The deviation

between the mid-afternoon surface temperature (measured by satellite) and the maximum air temperature (obtained from the meteorological ground network) (Ts–Ta), is related to the latent heat flux (Seguin *et al.*, 1991). The cumulative Σ(Ts–Ta), named stress-degree-day (Jackson *et al.*, 1977), has been proved to describe well the water stress of the vegetation. In this study, monthly values for (Ts–Ta) were calculated for each of the stations. For Ts, the average value of 2×2 pixels at the location of the meteorological station was calculated. The average monthly maximum air temperature was used for Ta values.

ENSO indices

The ENSO signal is measured through a number of indicators from the Pacific Ocean (Philander, 1990): Pacific sea surface temperature (SST), southern oscillation index (SOI) or outgoing long-wave radiation (OLR). SOI is related to the difference in sea level pressure between Papeete (Tahiti) and Darwin (Australia). OLR is used as an indicator of tropical rainfall linked to ENSO related convection in the Pacific Ocean area. SST is measured in four different regions of the Pacific Ocean between 5°N, and 5° or 10°S. Each region (Niño4, Niño3 and Niño1 + 2 zones) displays a slightly different pattern of change linked with the direction and the speed of warm water displacement in the Pacific Ocean (Philander, 1990). Sea surface temperature (SST) in the Pacific has been used in this study because it displays less noise than the southern oscillation index (SOI). We performed a first round of analyses using anomalies in SST for the four Niño zones. Generally, we found a stronger correlation between climate parameters (air temperature, humidity) or remote sensing variables (NDVI and Ts), and anomalies in SST for the Niño4 region (SST4 = 150°W–160°W, 5°N–5°S). The SST4 indicator was therefore used for the analyses in this study. The same indicator also showed the higher correlation in the PCA analysis by Anyamba & Eastman (1996). Note that the SST for the Niño3 zone has been used in studies analysing rainfall–ENSO teleconnections such as in Zimbabwe (Cane *et al.*, 1994).

METHOD

Pre-processing

Prior to the statistical analyses, all time series were standardized. Further calculations were performed on anomalies rather than on the original data. Monthly anomalies for each time series were calculated using the Z-score $(x_i - \mu)/(std)$ with x_i being the data value for a given month in year i, μ the mean data value for that month across all years and std the standard deviation of the data value for that month across all years. The time series of all variables were smoothed using a moving average filter over a 3-month period. As rainfall data were only available as total values per season for Tanzania, these data were standardized per season. The analysis of teleconnections with the rainfall data was performed separately for each season.

Teleconnections with climatic variables

Pearson correlation coefficients between the time series of anomalies of each of the climatic variables in East Africa and SST in the Niño4 zone in the Pacific were calculated for each meteorological station in the study area. As it was expected that changes in Pacific SST anomalies would have an effect on the climate in eastern Africa with a delay of several months, the correlation between time series of Pacific SST anomalies and climate anomalies in East Africa was calculated for lags of 1–12 months. Critical values for the correlation were calculated at the 0.95 and 0.99 level of significance.

Teleconnections with remote sensing variables

Pixel-wise correlation coefficients were calculated between Pacific SST anomalies and both East African NDVI and Ts anomalies. Lagged correlation was also used, with SST observed at steps from 1 to 12 months prior to the observations in East Africa. Correlation coefficients were also analysed at the 0.95 and 0.99 level of significance. The zones with a high positive or high negative correlation between NDVI or Ts anomalies in East Africa and Pacific SST anomalies were represented in a map.

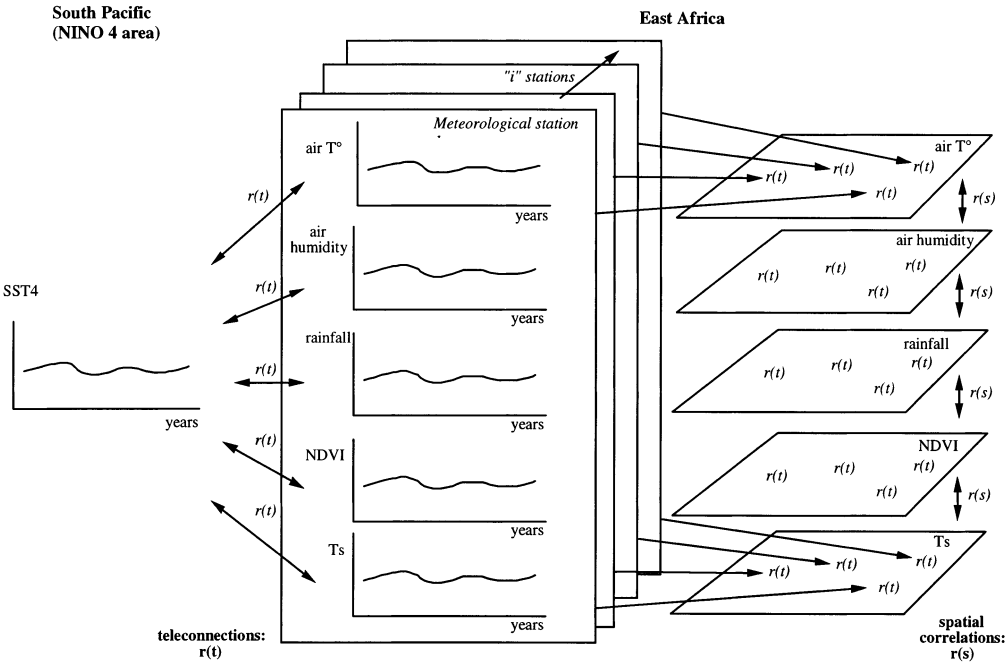

Fig. 2 Schematic representation of the methodology. First, for all stations, the teleconnection between Pacific SST4 and climate and remote sensing variables was computed. Secondly, the spatial correlations between values of teleconnections at all stations were computed for pairs of climate and remote sensing variables.

Testing the spatial coherence in teleconnections

The above analyses of teleconnections were performed independently for each variable and for each location (i.e. meteorological stations for the climate variables and AVHRR pixels for the remote sensing variables). To understand the combined effect on the ecosystem of the ENSO-induced inter-annual variability in the climate variables, we tested the spatial coherence in the response of these different variables to ENSO. Are these variables teleconnected to ENSO in the same way? Are there some specific climate and remotely sensed variables for which the response to ENSO is strongly coherent and in phase? Are there some locations in East Africa for which the teleconnections between ENSO and different ecosystem variables are observed with different time lags or at different magnitudes?

The location of each meteorological station was identified on the remote sensing data. Hence, the correlation coefficients between Pacific SST anomalies, and each of the remotely sensed variables were extracted for the locations corresponding to a meteorological station. Then, the spatial correlation between the strength of the teleconnections at every station was computed for all pairs of climate and remote sensing variables (Fig. 2). These spatial correlation coefficients represent the relationships in space between site-specific teleconnections with ENSO. They measure the level of spatial coherence in the response of the different ecosystem variables to ENSO. While these variables are mechanically linked (e.g. rainfall causes green vegetation growth which leads to an increase in vegetation index; green vegetation growth is associated with an increase in evapotranspiration which leads to a decrease in surface temperature) their patterns of teleconnection are not necessarily in phase and of the same magnitude. Different time lags were used to test whether there is a delayed response to ENSO in the remotely sensed variables as compared to the climate variables measured on the ground.

The above analysis will only test the spatial coherence in the way pairs of climate and/or remote sensing variables are teleconnected to ENSO. It is also interesting to identify spatial patterns of teleconnections based on the combination of all climate and remote sensing variables. For that purpose, we applied a multivariate clustering technique to regroup the stations according to the patterns of teleconnections with SST4 for all the ecosystem variables examined in this study.

RESULTS

Teleconnections with climate data

Most correlation values between Pacific SST anomalies and air temperature (maximum, minimum and average) measured at the East African stations are positive and highly significant ($P < 0.005$) (Fig. 3). As an example, a time–series of T_{avg} and SST4 anomalies is shown for Bujumbura in Fig. 4. For all three temperature variables, the highest correlation with SST4 anomalies is found in central Tanzania. The correlation between each of the air temperature variables and SST4 is maximal for a time lag of 4–8 months. For T_{min}, two stations do not show a significant correlation with SST4: the stations of Bukoba and Mwanza bordering Lake Victoria (Fig. 3). For the 12 meteorological stations in the study area, during the 1981–94 period, the three air temperature variables had higher values when SST4 anomalies were positive (with a 6-month time lag) as compared to the values for the years when SST4 anomalies were negative (Fig. 5a,b,c). Temperatures rose on average by 0.31 °C (T_{max}), 0.28 °C

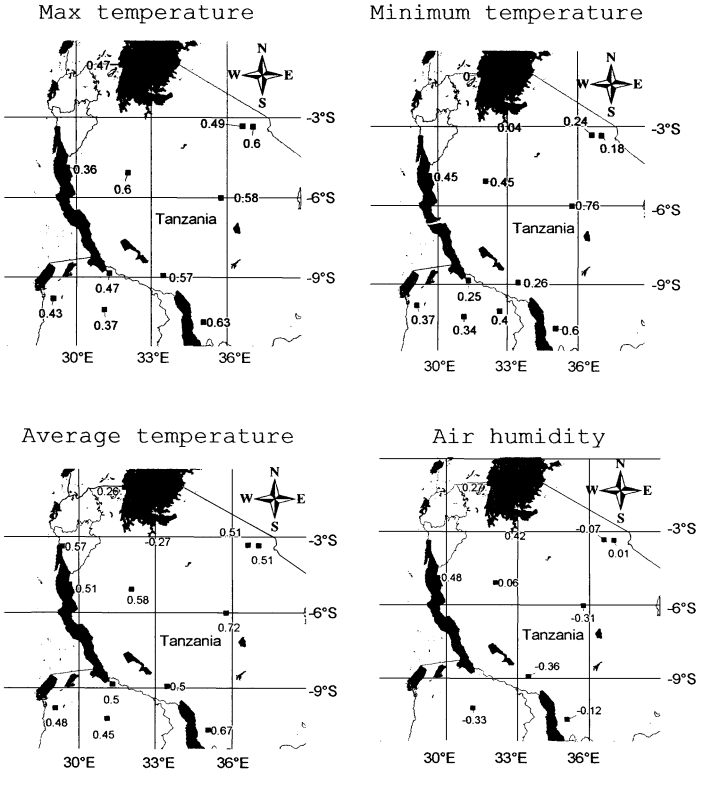

Fig. 3 Correlation coefficients (R) for teleconnections between, on one hand, monthly values of T_{max}, T_{min}, T_{avg} and relative air humidity in Zambia (1981–94) and Tanzania (1981–91) and, on the other hand, sea surface temperature (SST4) of the Pacific Ocean, for a 6-month time lag.

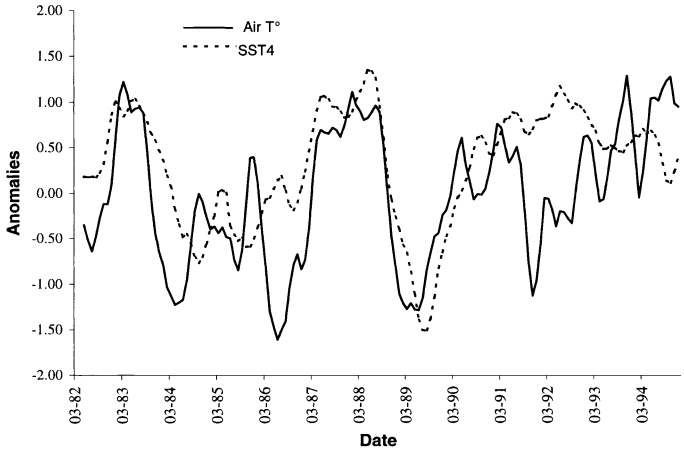

Fig. 4 Time series of SST4 anomalies and average air temperature anomalies at Bujumbura. The air temperature data are displayed with a 6-month time lag compared to the SST4 observations.

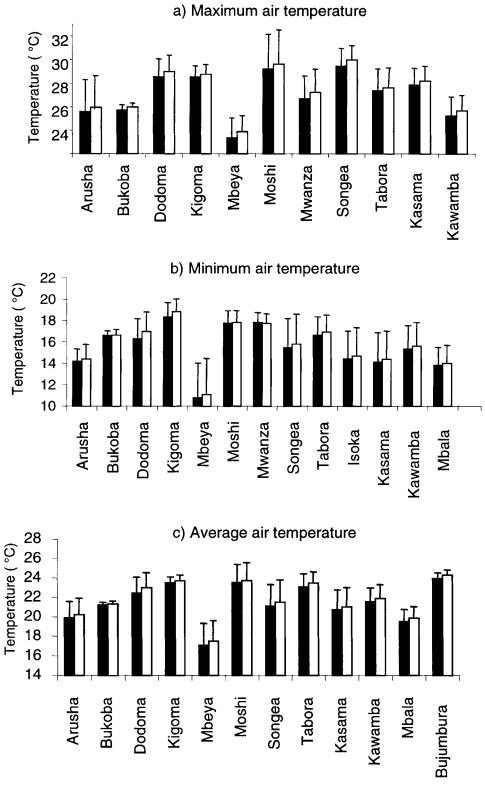

Fig. 5 Average values for: (a) T_{max}, (b) T_{min} and (c) T_{avg} at meteorological stations in Tanzania (1981–91) and in Zambia (1981–94) during periods with positive SST4 anomalies (in black) and periods with negative SST4 anomalies (in white).

(T_{avg}) and 0.26 °C (T_{min}) during warm ENSO events. The correlation between SST4 anomalies and air humidity is significant and positive in northern Tanzania (Mwanza, Bukoba) and north-western Tanzania (Kigoma), but is negative for all the other areas (Fig. 3). Moreover, the lag of the teleconnection between the SST4 anomalies and humidity is different for the two regions. In the first region (north-western Tanzania: Mwanza, Bukoba and Kigoma), the positive correlation is maximum for a 6-month time lag while, in the second region (south-eastern Tanzania and northern Zambia), the correlations reach the highest negative values for a 10-month time lag. This is probably related to differences in rainfall patterns between the north and the south of the study area. Thus, contrary to air temperature, there is not a single, region-wide effect of ENSO for the variable 'air humidity', but rather different effects for different locations. The increase in humidity in the north-western stations during ENSO warm events is 2–3%. However, this increase is not statistically significant as there are only a few meteorological stations in this region.

In Tanzania, teleconnections between SST4 and rainfall are analysed per season. For a number of stations with a bimodal rainfall pattern, the correlation between SST4 anomalies and anomalies for the long rainy season (March–May) is statistically significant and negative, which suggests that a warm ENSO event

Table 1 Correlation coefficients for teleconnections with SST4 anomalies for all stations. In bold: correlation values with $P < 0.01$. Ts = surface brightness temperature, NDVI = normalized difference vegetation index, T_{max} = monthly average of maximal air temperature, T_{min} = monthly average of minimum air temperature, T_{avg} = monthly average of air temperature, humidity = air humidity (Ts–Ta) = difference between the mid-afternoon surface temperature measured by satellite and the maximum air temperature, Roctdec = rainfall during the period from October to December, Rdecfeb = rainfall during the period from December to February, Rmarmay = rainfall during the period from March to May. The lag M is indicated between brackets (month)

	Ts (6 M)	NDVI (6 M)	T_{max} (6 M)	T_{min} (6 M)	T_{avg} (6 M)	Humidity (6 M)	(Ts–Ta) (6 M)	Roctdec (1 M)	Rdecfeb (5 M)	Rmarmay (4 M)
Arusha	–0.09	**–0.24**	**0.49**	**0.24**	**0.51**	–0.07	**–0.37**	0.23		–0.51
Bukoba	**–0.49**	0.07	**0.47**	0.00	**0.26**	**0.27**	**–0.72**	0.19		0.19
Dodoma	–0.10	**–0.24**	**0.58**	**0.76**	**0.72**	**–0.31**	**–0.44**		–0.10	
Kigoma	**–0.52**	–0.08	**0.36**	**0.45**	**0.51**	**0.48**	**–0.57**	**0.63**		**–0.79**
Mbeya	**–0.30**	**–0.22**	**0.57**	**0.26**	**0.50**	**–0.36**	**–0.66**		0.14	
Moshi	–0.17	–0.12	**0.60**	0.18	**0.51**	0.01	**–0.49**	0.30		–0.30
Mwanza	**–0.49**	**0.24**	0.14	0.18	0.18	**0.42**	**–0.53**	0.27		
Songea	**–0.22**	–0.01	**0.63**	**0.60**	**0.67**	–0.12	**–0.62**		0.02	
Tabora	**–0.43**	–0.13	**0.60**	**0.45**	**0.58**	0.06	**–0.77**			
Isoka	–0.21	–0.11		**0.40**				0.01	–0.30	–0.08
Kasama	**–0.34**	0.04	**0.37**	**0.34**	**0.45**	**–0.33**	**–0.47**	0.01	0.52	–0.35
Kawamba	**–0.32**	–0.21	**0.43**	**0.37**	**0.48**		**–0.47**	0.04	0.01	0.20
Mbala	**–0.45**	–0.10	**0.47**	**0.25**	**0.50**		**–0.58**	0.27	0.29	–0.32
Bujumbura	**–0.42**	0.01			**0.57**			–0.21	–0.71	–0.57

is associated with drier conditions during that season. The time lag involved was shorter than found for other parameters. Rainfall during the main wet season seems to be influenced by ENSO with a delay of 3–4 months. For the short rainy season, the teleconnection is not significant in Tanzania, but tends to be positive with a shorter time lag. For the other meteorological stations, only Bujumbura has a strong negative correlation between monthly precipitation anomalies and SST4 anomalies, with a delay of 3–4 months (Table 1). This finding still needs to be confirmed with longer-term rainfall data.

Teleconnections with remote sensing data

Correlation coefficients between both NDVI and Ts anomalies and the ENSO index were found to be strongest for a time lag of 6–8 months. Correlation values for the NDVI-SST4 teleconnection vary in space between –0.70 and +0.55. Thirty per cent of the values are negative and statistically significant ($P < 0.005$) and 0.6% of the correlations are positive and significant (Fig. 6a). For the teleconnection between Ts and SST4, 65% of the area shows a significant negative correlation, but only 0.02% of the pixels have a significant positive correlation (Fig. 6b). Again, for these two variables, there is not a single, region-wide effect of ENSO but rather different effects for different locations.

To understand better the pattern of teleconnection between Pacific SST4 and the remotely sensed land surface variables, a land cover map for Africa was used to determine the different vegetation types in the area. We used the global land cover map at 1 km^2 resolution produced by the IGBP (Loveland & Belward, 1999). In the north-western part of the study area, there is a strong negative correlation between NDVI and SST4 (Fig. 6a), meaning that warm ENSO events are associated with a lower-than-usual NDVI, thus suggesting a lower net primary production. Towards the south of this area, on the western side of Lake Tanganyika, the negative correlation values are smaller, but still significant. The north-western area is covered by evergreen tropical forest, gradually changing into woody savanna towards the south. Another area with pronounced negative correlation values

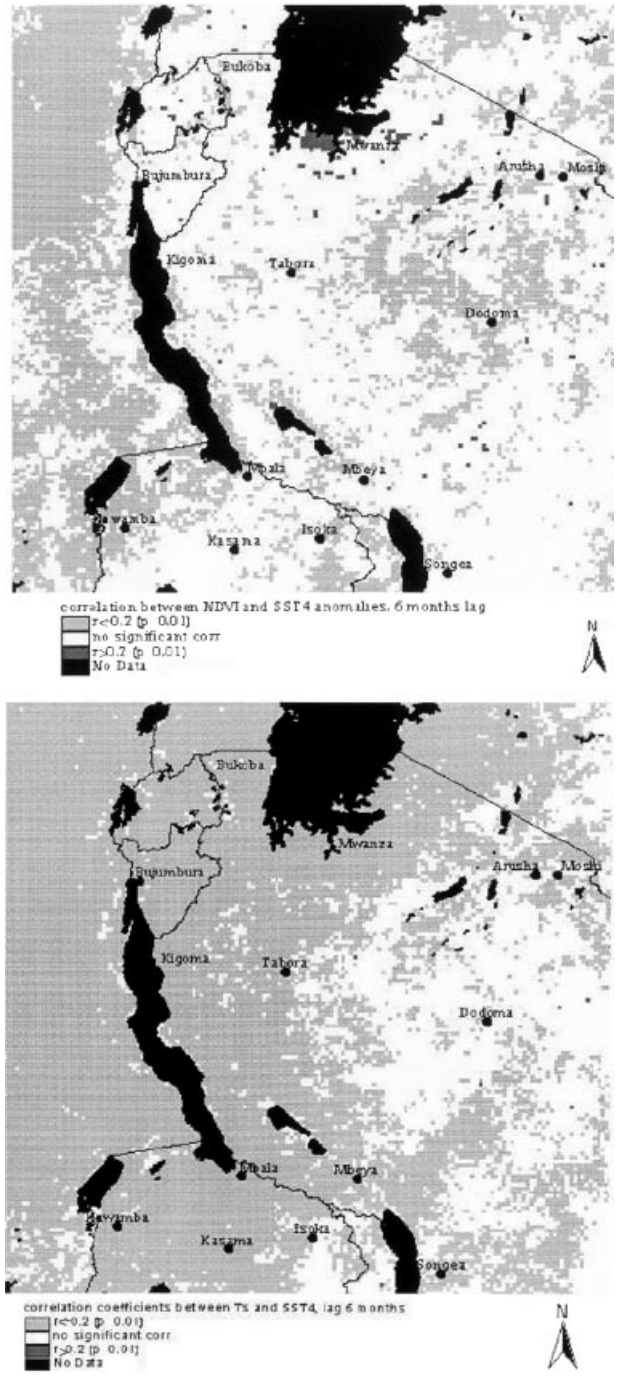

Fig. 6 Maps showing pixel-wise correlation coefficients for the teleconnections between SST4 anomalies and: (a) NDVI anomalies and (b) Ts anomalies, with a 6-month time lag. Only the values of the correlation coefficients which are significant at the level 0.01 are represented.

Table 2 Spatial correlation coefficients between teleconnection values for pairs of variables. The lag used for all variables was 6 months. In italics: $P < 0.05$; in bold: $P < 0.01$

	Ts	NDVI	T_{max}	T_{min}	T_{avg}	Humidity	(Ts–Ta)
Ts	1	*–0.595*	*0.567*	0.391	*0.569*	*–0.697*	*0.598*
NDVI		1	*–0.643*	–0.379	**–0.656**	0.547	–0.239
T_{max}			1	0.343	**0.753**	*–0.570*	–0.228
T_{min}				1	**0.820**	–0.374	0.158
T_{avg}					1	*–0.580*	0.132
Humidity						1	–0.238
(Ts–Ta)							1

for the NDVI-SST4 teleconnection is found in the Maasai steppe, south of Arusha (Fig. 6a). This is a relatively flat area dominated by savanna and some grassland vegetation. There is a small area south of Lake Victoria and close to Mwanza, characterized by a strong positive correlation between NDVI and SST4, suggesting that warm ENSO events are associated with an increase in net primary production of the vegetation. Other areas with a positive but weak teleconnection between NDVI and SST4 are found west of Lake Victoria and near Lake Tanganyika, north-east of Kigoma, in areas supporting a grassland vegetation or a mixture of cropland and natural vegetation. We see in this case that there is no perfect correspondence between land cover types and the pattern of ENSO teleconnection of NDVI as different grassland areas are affected by both positive and negative correlations with SST4. In the remaining areas, the teleconnection between NDVI and SST4 is not significant and no clear impact of ENSO events on vegetation can be observed.

The correlation coefficients for Ts–SST4 teleconnections are largely negative (Fig. 6b), implying that a positive Pacific SST4 anomaly will cause lower than usual surface temperatures (Ts) in East Africa about 6–8 months later. The area that shows the strongest teleconnection between Ts and SST4 is found in the north-western part of the study area, in the evergreen broadleaved forest. Further to the south, the teleconnections are weaker, but significant negative correlation values are found for the area around Lake Victoria, around Lake Tanganyika and down to Lake Rukwa. In the centre and towards the east of the study area, correlation values are insignificant. For a few pixels in the eastern part of the study area, covered by woody savanna, significant but weak positive teleconnections for Ts are found.

Teleconnections with Pacific SST for the (Ts–Ta) variable are negative for all stations and are strongest for a time lag of 6 months. Thus, for years with positive ENSO anomalies (Ts–Ta) values are smaller than usual, suggesting that evapotranspiration is increased for all meteorological stations.

Spatial coherence in teleconnections

In general, the teleconnections with Pacific SST of the different climate and remotely sensed variables are spatially coherent (Table 1), with notable exceptions concerning the NDVI teleconnection, which measures the response of vegetation to the ENSO-induced climate variability. First, the spatial correlation values for teleconnections of pairs of climate variables will be examined. Secondly, the spatial correlation between the teleconnections for the two remotely sensed variables is analysed; and thirdly, the spatial correlation between the teleconnections for pairs of one climate and one remote-sensing variable is examined. Results are presented in Table 2. These analyses were conducted using teleconnection data from all the stations.

As could be expected, the three variables related to air T° (maximum, minimum and average air T°) are teleconnected to SST4 in the same way, with the spatial correlations being positive and significant at $P < 0.005$ (Fig. 7a). These three air T° variables and air humidity are also teleconnected with ENSO in a similar way but with the opposite sign in the case

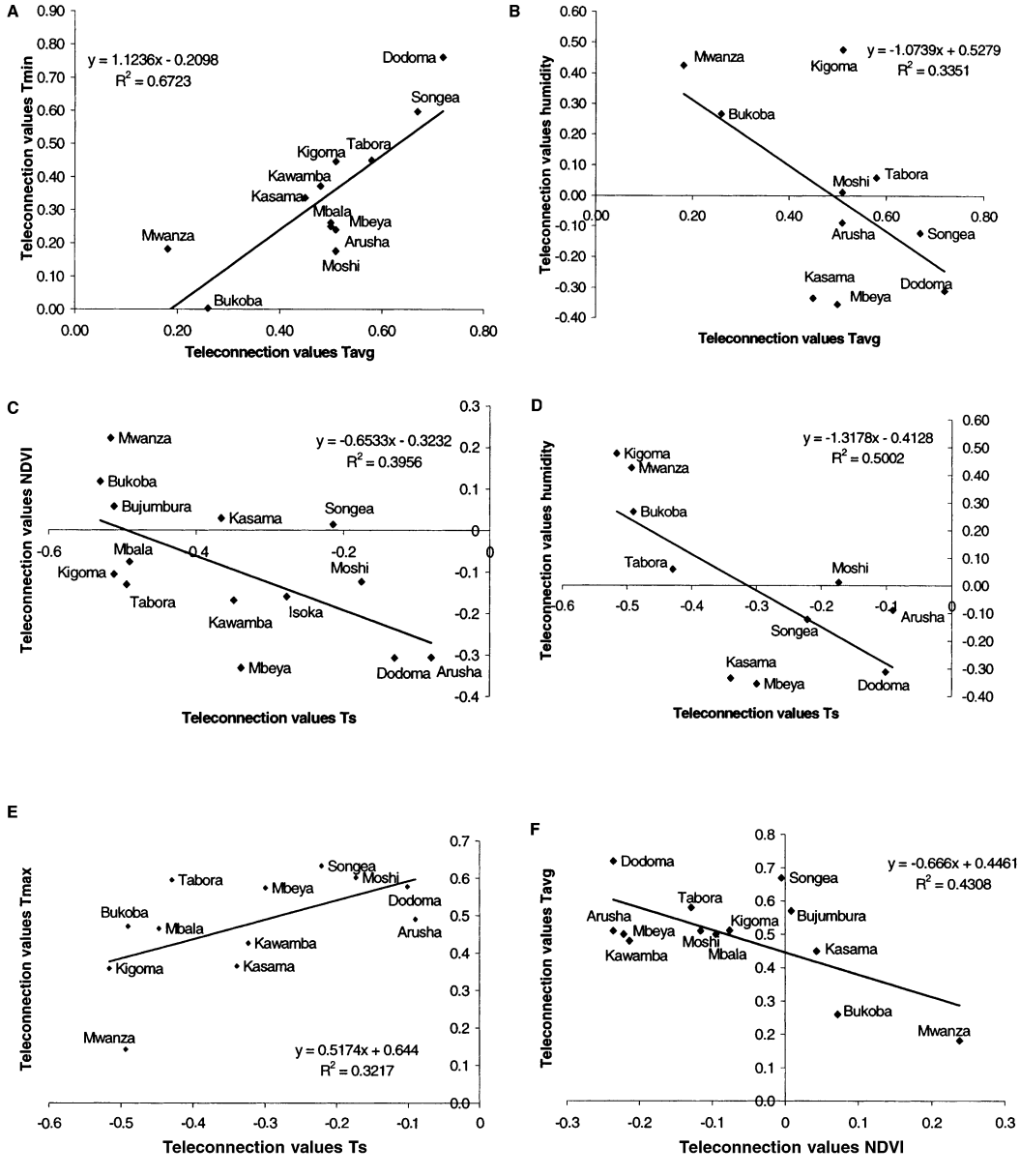

Fig. 7 Scatterplots of the teleconnection values (i.e. correlations between Pacific SST4, and climate and remote sensing variables for each station) for pairs of climate and remote sensing variables for all stations: (A) average and minimum air temperature, (B) average air temperature and air humidity, (C) Ts and NDVI, (D) Ts and air humidity, (E) Ts and maximum air temperature, and (F) NDVI and average air temperature.

of air humidity — spatial correlations significant and negative (Fig. 7b). Two areas may be distinguished: the stations in the north-eastern part of the study area (Bukoba, Mwanza), which have high teleconnections with humidity and lower teleconnections with air T°, and the stations in the south-western part of the study area (Dodoma, Songea, Mbeya), which show

the inverse combination. Note that the teleconnections in Kigoma between SST4 and T_{min}, T_{avg} and relative air humidity are all particularly high compared to the other stations. A significant spatial correlation was also found between teleconnections for rainfall during the period March–May and teleconnections for average air temperature.

The spatial correlations between the NDVI-SST4 and Ts–SST4 teleconnections are significant and generally negative (Fig. 7c). The negative value for the spatial correlation between NDVI and Ts teleconnections is expected as, in water-limited ecosystems, an increase in photosynthetically active green biomass is associated with a reduction in surface resistance to evapotranspiration, a larger latent heat flux and therefore a lower surface temperature (Lambin & Ehrlich, 1996). Accordingly, a positive teleconnection between NDVI and SST4 is expected to be associated with a negative teleconnection between Ts and SST4. This is verified for most of our study area, except for the north-western part of the region, which is dominated by evergreen forests (Fig. 6a,b). Over evergreen forests, where there is no moisture availability constraint, both the NDVI–SST4 and Ts–SST4 teleconnection values are strongly negative. Thus, depending on land cover and ecosystem constraints, the sign of the relationship between the NDVI and Ts teleconnections may be inverted. Accordingly, it is difficult to identify a unique relationship for the entire study area between the teleconnections of NDVI and Ts with SST4. As for the climate variables discussed above, there is generally a difference between the north-western stations of the study area (Mwanza, Bukoba, Bujumbura and Kigoma) and the south-eastern stations (Dodoma, Arusha, Moshi and Songea) in the NDVI and Ts teleconnection with SST4 (Fig. 7c).

Teleconnections between SST4 and Ts measured by remote sensing show, in general, a good spatial correlation of the SST4 teleconnections with the climate variables. The teleconnection patterns for Ts and air humidity correlate best, with a negative sign (Fig. 7d). Thus, during a positive ENSO event, air humidity is higher in regions that have lower Ts, i.e. in regions characterized by a high surface evapotranspiration. The north-eastern stations are again well separated from the south-western stations. As could be expected, there is a good spatial correlation between Ts and (Ts–Ta). Spatial correlations between the SST4 teleconnections with Ts and air temperature (T_{max} and T_{avg}) variables are strong and positive (Fig. 7e), while NDVI teleconnections are negatively correlated with air temperature variables (Fig. 7f). Rainfall teleconnection data show a negative spatial correlation for teleconnections with Ts and rainfall in December–February. Only stations that have a unimodal pattern are taken into account here. Increase in rainfall increases surface moisture, which increases evapotranspiration and therefore decreases surface temperature. The station of Bujumbura does not comply with this correlation pattern. The spatial patterns of SST4 teleconnections of NDVI and air humidity seem to be positively correlated for all stations except for Kigoma, Kasama and Songea. The overall relationship is not statistically significant. Against the expectations, no overall spatial correlation was found between NDVI and rainfall teleconnections. Meteorological stations with a bimodal rainfall pattern in the north-east of the study area display a weak (not significant) positive correlation with NDVI teleconnections for the main rainy season in March–May. For the stations with a unimodal rainfall season in Zambia, the spatial correlation between NDVI and rainfall teleconnections (March–May) is significant ($P < 0.05$) and negative.

Clustering of stations based on their pattern of teleconnections with SST4

A multivariate clustering technique allows regrouping of the stations according to their teleconnection values for the entire set of climate and remote sensing variables. A 6-month time lag was used for the teleconnections with all the variables. Teleconnections for rainfall data were not used in this analysis due to the coarse temporal resolution of the rainfall data. A first separation into two clusters of stations is made between all lakeside stations (Mwanza, Bukoba, Bujumbura and Kigoma) and the remaining stations. All lakeside stations have a strong positive teleconnection between SST4 and air humidity. Air humidity was not available for Mbala, but teleconnections with other variables

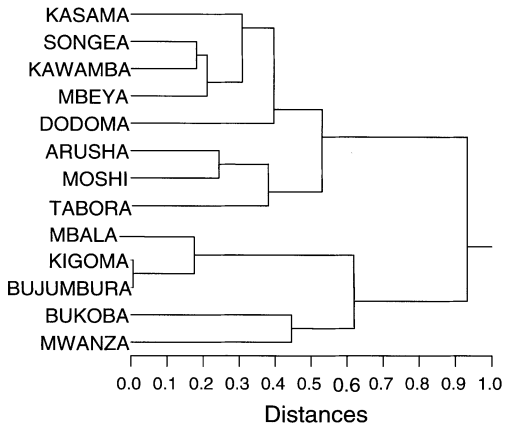

Fig. 8 Cluster tree grouping the stations based on their teleconnection values with SST4 (with a 6-month lag) for Ts, NDVI, T_{max}, T_{min}, T_{avg}, humidity and (Ts–Ta).

follow the same pattern as the other lakeside stations. The lakeside stations are further characterized by strong negative teleconnections with Ts and no teleconnection with NDVI (except Mwanza). Moderate positive teleconnection values were found for air temperature variables for the stations situated near Lake Tanganyika, but the stations near Lake Victoria do not have a teleconnection with the temperature variables. (Fig. 8). Thus, ecosystems located near the great east African lakes display a specific pattern of teleconnections compared to other locations. This reveals the importance of the lakes on local climate conditions. The stations in the drier part of the study area, lying on the central plateau or in the south (Kasama, Songea, Kawamba, Mbeya and Dodoma), are also grouped together. The area has a unimodal rainfall pattern and naturally supports a savanna vegetation which, in certain zones, is converted to cropland. The stations are characterized by a strong negative teleconnection between SST4 and air humidity. Furthermore, the stations display a negative teleconnection with NDVI and a negative teleconnection with Ts (moderate values). The remaining stations of Arusha, Moshi and Tabora are grouped together based on the absence of any teleconnection with air humidity. Teleconnections with remote sensing variables are also insignificant, while teleconnections with maximum and average air temperature are consistently high and positive. Arusha and Moshi are both situated in the north-east of the study area, at the footslopes of Mount Meru and Mount Kilimanjaro, respectively. Rainfall pattern is bimodal and the area supports a woody savanna vegetation.

DISCUSSION AND CONCLUSION

Teleconnections with ENSO are observed for all climate and land surface variables analysed here. This confirms the ENSO impact on the climatic and ecological variability in East Africa. However, the pattern of teleconnections is much more complex than generally assumed, both in terms of spatial distribution and impact on different ecosystem variables. Air temperature is clearly positively linked with ENSO in the entire study area. The average temperature increase in this area during warm ENSO events was +0.28 °C during the 1981–94 period. The correlation with Pacific SST4 is particularly strong for air temperature in eastern Tanzania. This could be linked to the proximity of East Tanzania to the Indian Ocean where SST warming is also observed during ENSO events (Monastersky, 1994; Toure, pers. comm.). Significant teleconnections between rainfall and SST in the Pacific Ocean were found for very few stations in this study. The weak teleconnection with rainfall can be linked to the high spatial and temporal variability of rains, which are strongly influenced by local conditions, and to the short period considered here (1981–94) compared to previous studies dealing mainly with rainfall (Nicholson, 1996). Our results suggest that the relative air humidity could be a more sensitive and more easily detectable indicator of climate teleconnections than rainfall.

Most of the previous studies have dealt mainly with one climate variable at a time, mostly rainfall. One of the major findings of this study is that several other climate and land surface attributes show a partial correlation with the fluctuation of the Pacific SST4 index. These different variables are not all teleconnected to ENSO in the same way, which leads to a complex impact of ENSO on the ecosystem. The sea surface temperature anomalies in the

Pacific Ocean induce changes in climate variables such as air temperature and air humidity and rainfall. These ENSO-driven changes in climate induce changes in vegetation activity, as measured by changes in NDVI and changes in Ts and (Ts–Ta), which indicate changes in surface moisture and evapotranspiration. The exact response of vegetation to the ENSO-induced climate variations depends on land cover. There were no clear indications that there is an additional time lag for the teleconnections of remote sensing variables as compared to the teleconnections of climate parameters (except rainfall), which suggests a rapid response of vegetation to changes in climate conditions. The few results obtained with rainfall data suggest that the response of rainfall to SST4 anomalies is more rapid (3–4 months) than is the case for other climate variables.

The second major finding of this study is that the ENSO impact is highly differentiated in space. Many previous studies have postulated a single, region-wide impact of ENSO. In reality, the direction, magnitude and timing of this impact is controlled by the climate system at a regional scale and at a more local scale, i.e. as influenced by the presence of large lakes, local topography or proximity to the coast. Surface attributes, as determined by geology, soils and vegetation might also influence the magnitude and the time lag of the ENSO impact. Hence, different zones are recognized in the study area, each subject to different combinations of ENSO induced climate variations. The lakes region in the north-west is one zone, the plateau in the centre and south-east of the study area is a second one and the more temperate stations in the north-east form a third zone. For example, during warm ENSO phases, the Lake Victoria area showed warmer and more humid conditions with an increased vegetation activity while the central and southern part of the study area showed warmer, but drier conditions with a decreased vegetation activity. The area west of Lake Tanganyika is characterized by poor vegetation conditions during warm ENSO events.

Our study area is situated at the interface between main centres of teleconnection between climate variables and SST of the Pacific Ocean. These centres have opposite signs for the teleconnection between SST4 and rainfall: a positive correlation in the east-equatorial area and a negative correlation in southern Africa (Rasmusson & Arkin, 1985; Ropelewski & Halpert, 1987). Within each of these broad zones, different weather systems interact on finer spatial scales. The main weather system in East Africa is associated with the Intertropical Convergence Zone (ITCZ), a belt of low pressure following 6 weeks behind the sun as it moves south and north of the equator. The southward movement brings north-easterly prevailing winds to Tanzania from November to May. From June to September, the south-west monsoon brings relatively cool, dry weather. The wetter climate of the Congo is influenced by the eastern winds from the Atlantic Ocean. These patterns are influenced by local phenomena, such as rain shadow areas created in the vicinity of mountain ranges. Lake Victoria, for example, produces its own convergence zone and affects certain areas by increasing precipitation in the dry season. The difference in time lag for the maximum correlation between relative air humidity and SST4 in the north and the south of the study area is probably linked to the Intertropical Convergence Zone that drives the rainy season in both areas with a lag of a few months.

A third finding of the study is that ENSO is not the only source of inter-annual variability in climate conditions in the region, as none of the correlation coefficients measured in this study were very high (in the range of 0.3–0.6). The mechanisms behind the teleconnections with SST are still hypothetical. The SST4 index is measured in the part of the Pacific that is geographically closer to Africa. Only SST fluctuations in the Pacific Ocean have been considered here although it could be argued that the ENSO-induced SST fluctuations in the Indian and Atlantic Ocean might be more strongly teleconnected with climate variability in Africa (Trenberth, 1991; Nicholson, 1996; Charles *et al.*, 1997). A further study should investigate the teleconnections with those neighbouring oceans as well.

As modelling and forecasting efforts of global phenomena such as ENSO are underway, the detailed study of teleconnections between regional African climate parameters and ENSO improves the prospect for partial forecasting of

ENSO impacts on agriculture, fisheries or health. Although the results on rainfall teleconnections in the study area do not allow us to make firm statements on the usability of rainfall teleconnections for the forecasting of ENSO impacts it is shown that other variables, such as air temperature, air humidity or vegetation activity, are significantly correlated to ENSO. These teleconnections have a potential for forecasting as, for some resources, small changes in climate conditions have an important effect on ecosystem functions. For example, small changes in air temperature may have a significant impact on the thermic stratification of tropical lakes. Vegetation response to ENSO integrates the impact of several climate parameters.

Considerable work remains to be done on the identification of teleconnections in Africa for many other climate variables such as wind patterns, cloudiness or radiation. Comprehensive time series for weather variables for a large number of stations, widely distributed in Africa, are often lacking. Remote sensing data may partially fill this gap for the recent years and for land surface attributes. A better understanding of the mechanisms of the teleconnections would, however, have to rely on comprehensive climate data, including several extreme ENSO phases.

ACKNOWLEDGMENTS

This work is part of a multidisciplinary research project financed by the Prime Minister's Office — Federal Office for Scientific, Technical and Cultural Affairs, Belgium (contract CG/DD/10).

REFERENCES

Anyamba, A. & Eastman, J.R. (1996) Inter-annual variability of NDVI over Africa and its relation to El Niño/Southern Oscillation. *International Journal of Remote Sensing*, **17**, 2533–2548.

Asrar, G., Myneni, R.B. & Choudhury, B.J. (1992) Spatial heterogeneity in vegetation canopies and remote sensing of absorbed photosynthetically active radiation: a modelling study. *Remote Sensing of Environment*, **41**, 85–103.

Batista, G.T., Shimabukuro, Y.E. & Lawrence, W.T. (1997) The long-term monitoring of vegetation cover in the Amazonian region of northern Brazil using NOAA-AVHRR data. *International Journal of Remote Sensing*, **18**, 3195–3210.

Cane, A.C., Eshel, G. & Buckland, R.W. (1994) Forecasting Zimbabwean maize yield using eastern equatorial Pacific sea surface temperature. *Nature*, **370**, 204–205.

Carlson, T.N., Perry, E.M. & Schmugge, T.J. (1990) Remote sensing of soil moisture availability and fractional vegetation cover for agricultural fields. *Agriculture and Forest Meteorology*, **52**, 45–69.

Charles, C.D., Hunter, D.E. & Fairbanks, G. (1997) Interaction between the ENSO and the Asian monsoon in a coral record of tropical climate. *Science*, **277**, 925–928.

Chen, D., Zebiack, S.E., Busalacchi, A.J. & Cane, M.A. (1995) An Improved Procedure for El Niño forecasting: implication for predictability. *Science*, **269**, 1699–1702.

Davenport, M.L. & Nicholson, S.E. (1993) On the relation between rainfall and the normalised difference vegetation index for diverse vegetation types in East Africa. *International Journal of Remote Sensing*, **14**, 2369–2389.

Diaz, H.F. & Kiladis, G.N. (1992) Atmospheric teleconnections associated with the extreme phases of the southern oscillation. *El Niño: historical and paleoclimatic aspects of the southern oscillation* (ed. by H.F. Diaz and V. Markgraf), pp. 2–28, Cambridge University Press, Cambridge.

Eklundh, L. (1998) Estimating relations between AVHRR NDVI and rainfall in East Africa at 10-day and monthly time scales. *International Journal of Remote Sensing*, **19**, 563–568.

Farmer, G. (1988) Seasonal forecasting of the Kenya coast short rains 1901–84. *Journal of Climatology*, **8**, 489–497.

Gucinski, H., Lackey, R.T. & Spence, B.C. (1990) Global climate change: policy implications for fisheries. *Fisheries*, **15**, 33–38.

Holben, B.N. (1986) Characteristics of maximum-value composite images from temporal AVHRR data. *International Journal of Remote Sensing*, **7**, 1417–1434.

Houghton, J.T., Jenkins, G.J & Ephraums J.J (eds) (1990) *Climate Change. The IPCC scientific assessment. Intergovernmental panel on climate change*, 364 pp. Cambridge University Press, Cambridge.

Jackson, R.D., Reginato, R.J. & Idso, S.B. (1977) Wheat canopy temperature: a practical tool for evaluation water requirements. *Water Resources Research*, **13**, 651–656.

Kumar, M. & Monteith, J.L. (1981) Remote sensing of plant growth. *Plants and the Daylight Spectrum* (ed. by H. Smith), pp. 133–144, Academic Press, New York.

Lambin, E.F. & Ehrlich, D. (1996) The surface temperature–vegetation index space for land cover and land-cover change analysis. *International Journal of Remote Sensing*, **17**, 463–487.

Linthicum, K.J., Anyamba, A., Tucker, C.J., Kelley, P.W., Myers, M.F. & Peters, C.J. (1999)

Climate and satellite indicators to forecast Rift valley fever epidemics in Kenya. *Science*, **285**, 397–400.

Loveland, T.R. & Belward, A.S. (1999) The IGBP-DIS global 1 km land cover data set, DISCover: first results. *International Journal of Remote Sensing*, **18**, 3289–3296.

Monastersky, R. (1994) Twin of El Niño found in Indian Ocean. *Science News*, **146**, 442.

Myneni, R.B., Los, S.O. & Tucker, C.J. (1996) Satellite-based identification of linked vegetation index and sea surface temperature anomaly areas from 1982 to 1990 for Africa, Australia and South America. *Geophysical Research Letters*, **23**, 729–732.

Nicholson, S.E. (1996) A review of climate dynamics and climate variability in Eastern Africa. *The Limnology, Climatology and Paleoclimatology of the East African Lakes* (ed. by T.C. Johnson & E.O. Odada), pp. 25–56. Gordon & Breach Publishers, Amsterdam.

Nicholson, S.E. & Entekhabi, D. (1986) The quasi-periodic behaviour of rainfall variability in Africa and its relationship to the Southern Oscillation: *Journal of Climate and Applied Meteorology*, **34**, 311–348.

Myneni, R.B., Maggion, S., Iaquinta, J., Privette, J.L., Gobron, N., Pinty, B., Kimes, D., Verstraete, M. & Williams, D. (1995) Optical remote sensing of vegetation: modelling, caveats and algorithms. *Remote Sensing of Environment*, **51**, 169–188.

Ogallo, L. (1987) Relationships between seasonal rainfall in East Africa and the Southern Oscillation. *Journal of Climatology*, **7**, 1–13.

Philander, S.G. (1990) *El Niño, la Niña, and the Southern Oscillation*. Academic Press Inc., San Diego.

Price, J.C. (1984) Land surface temperature measurements from the split-window channels of the NOAA 7 Advanced Very High Resolution Radiometer. *Journal of Geophysical Research*, **85**, 7231–7237.

Rasmusson, E.M. & Arkin, P.A. (1985) Inter-annual climate variability associated with the El Niño/Southern Oscillation. *Coupled Ocean–Atmosphere Models* (ed. by J.C. Nihoul). *Elsevier Oceanographic Series*, **40**, 697–725.

Richard, Y. & Poccard, I. (1998) A statistical study of NDVI sensitivity to seasonal and inter-annual rainfall variations in Southern Africa. *International Journal of Remote Sensing*, **19**, 2907–2920.

Ropelewski, C.F. & Halpert, M.S. (1987) Global and regional scale precipitation and temperature patterns associated with El Niño-Southern Oscillation. *Monthly Weather Reviews*, **15**, 1606–1626.

Seguin, B., Lagouarde, J.P. & Savane, M. (1991) The assessment of regional crop water conditions from meteorological satellite thermal infrared data. *Remote Sensing of Environment*, **35**, 141–148.

Smith, P.M., Kalluri, S.N.V., Prince, S.D. & DeFries, R. (1997) the NOAA/NASA Pathfinder AVHRR 8-km land data set. *Photogrammetic Engineering & Remote Sensing*, **63**, 12–32.

Trenberth, K.E. (1991) General characteristics of El Niño-Southern Oscillation. *Teleconnection Linking Worldwide Climate Anomalies* (ed. by M.H. Glantz, R.W. Katz & N. Nicholls), pp. 13–42. Cambridge University Press, Cambridge.

Trenberth, K.E. & Shea, D.J. (1987) On the evolution of the Southern Oscillation. *Monthly Weather Review*, **115**, 3078–3096.

Verdin, J., Funk, C., Klaver, R. & Roberts, D. (1999) Exploring the correlation between Southern Africa NDVI and Pacific sea surface temperature: results for the 1998 maize growing season. *International Journal of Remote Sensing*, **20**, 2117–2124.